Chemical Research in Toxicology

ACS AuthorChoice

Article

pubs.acs.org/crt

Terms of Use

Ring-Opening of the γ-OH-PdG Adduct Promotes Error-Free Bypass by the *Sulfolobus solfataricus* DNA Polymerase Dpo4

Ganesh Shanmugam,[†,⊥,#] Irina G. Minko,[§,⊥] Surajit Banerjee,[†,⊥,▽] Plamen P. Christov,[†] Ivan D. Kozekov,[†] Carmelo J. Rizzo,[†,‡] R. Stephen Lloyd,[§,∥] Martin Egli,[‡] and Michael P. Stone*[,†,‡]

[†]Department of Chemistry, Center in Molecular Toxicology, Vanderbilt-Ingram Cancer Center, Vanderbilt Institute of Chemical Biology, and Center for Structural Biology, Vanderbilt University, Nashville, Tennessee 37235, United States

[‡]Department of Biochemistry, Center in Molecular Toxicology, Vanderbilt-Ingram Cancer Center, Vanderbilt Institute of Chemical Biology, and Center for Structural Biology, Vanderbilt University, Nashville, Tennessee 37235, United States

[§]Center for Research on Occupational and Environmental Toxicology, Oregon Health & Science University, Portland, Oregon 97239, United States

[∥]Department of Molecular and Medical Genetics, Oregon Health & Science University, Portland, Oregon 97239, United States

Supporting Information

ABSTRACT: Acrolein, a mutagenic aldehyde, reacts with deoxyguanosine (dG) to form 3-(2′-deoxy-β-D-*erythro*-pentofuranosyl)-5,6,7,8-tetrahydro-8-hydroxypyrimido[1,2-*a*] purin-10(3*H*)-one (γ-OH-PdG). When placed opposite deoxycytosine (dC) in DNA, γ-OH-PdG undergoes ring-opening to the N^2-(3-oxopropyl)-dG. Ring-opening of the adduct has been hypothesized to facilitate nonmutagenic bypass, particularly by DNA polymerases of the Y family. This study examined the bypass of γ-OH-PdG by *Sulfolobus solfataricus* Dpo4, the prototypic Y-family DNA polymerase, using templates that contained the adduct in either the 5′-CXG-3′ or the 5′-TXG-3′ sequence context. Although γ-OH-PdG partially blocked Dpo4-catalyzed DNA synthesis, full primer extension was observed, and the majority of bypass products were error-free. Conversion of the adduct into an irreversibly ring-opened derivative prior to reaction facilitated bypass and further improved the fidelity. Structures of ternary Dpo4·DNA·dNTP complexes were determined with primers that either were positioned immediately upstream of the lesion (preinsertion complexes) or had a 3′-terminal dC opposite the lesion (postinsertion complexes); the incoming nucleotides, either dGTP or dATP, were complementary to the template 5′-neighbor nucleotide. In both postinsertion complexes, the adduct existed as ring-opened species, and the resulting base-pair featured Watson−Crick hydrogen bonding. The incoming nucleotide paired with the 5′-neighbor template, while the primer 3′-hydroxyl was positioned to facilitate extension. In contrast, γ-OH-PdG was in the ring-closed form in both preinsertion complexes, and the overall structure did not favor catalysis. These data provide insights into γ-OH-PdG chemistry during replication bypass by the Dpo4 DNA polymerase and may explain why γ-OH-PdG-induced mutations due to primer−template misalignment are uncommon.

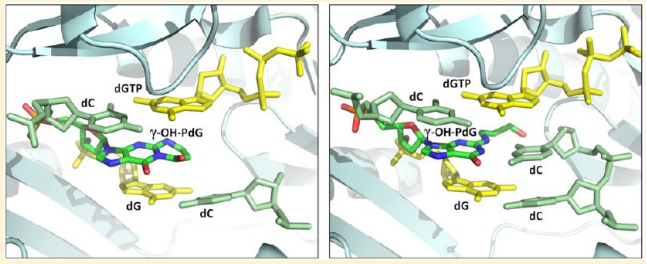

INTRODUCTION

Acrolein, the simplest α,β-unsaturated aldehyde, is both a product of common cellular processes, such as lipid peroxidation, and a widespread air pollutant.[1−5] Acrolein has been shown to induce mutations in mammalian and bacterial cells[6−10] and promote carcinogenesis in rats.[11] The principal adduct from the reaction of acrolein with DNA is 3-(2′-deoxy-β-D-*erythro*-pentofuranosyl)-5,6,7,8-tetrahydro-8-hydroxypyrimido[1,2-*a*]purin-10(3*H*)-one (γ-OH-PdG),[10,12−14] which is formed as a result of Michael addition of the N^2-amine of deoxyguanosine (dG) to yield the N^2-(3-oxopropyl)-dG adduct,[1] which further cyclizes with N1 (Scheme 1).

NMR spectroscopic analyses of DNA containing γ-OH-PdG[15−17] demonstrated that the adduct undergoes spontaneous ring-opening to the N^2-(3-oxopropyl)-dG or N^2-(3,3-dihydroxypropyl)-dG when positioned opposite deoxycytosine (dC) (Scheme 1). The modified base is in the *anti* orientation about the glycosyl bond and maintains Watson−Crick pairing, and its partially hydrated aldehydic group is located in the minor groove. The structure is remarkably different from that of DNA containing 3-(2′-deoxy-β-D-*erythro*-pentofuranosyl)-5,6,7,8-tetrahydropyrimido[1,2-*a*]purin-10(3*H*)-one (PdG), a model six-membered exocyclic adduct that is incapable of ring-opening. PdG tends to adopt a *syn* orientation and forms a pair with the opposing dC via the Hoogsteen face.[18−20]

The mutagenic properties of γ-OH-PdG have been investigated through intracellular replication of site-specifically adducted vector DNAs. The majority of the replication bypass

Received: June 1, 2013
Published: August 16, 2013

   dx.doi.org/10.1021/tx400200b | *Chem. Res. Toxicol.* 2013, 26, 1348−1360

Scheme 1. Reaction of Acrolein with dG and the Ring-Opening Chemistry of the γ-OH-PdG Adduct Opposite dC in DNA

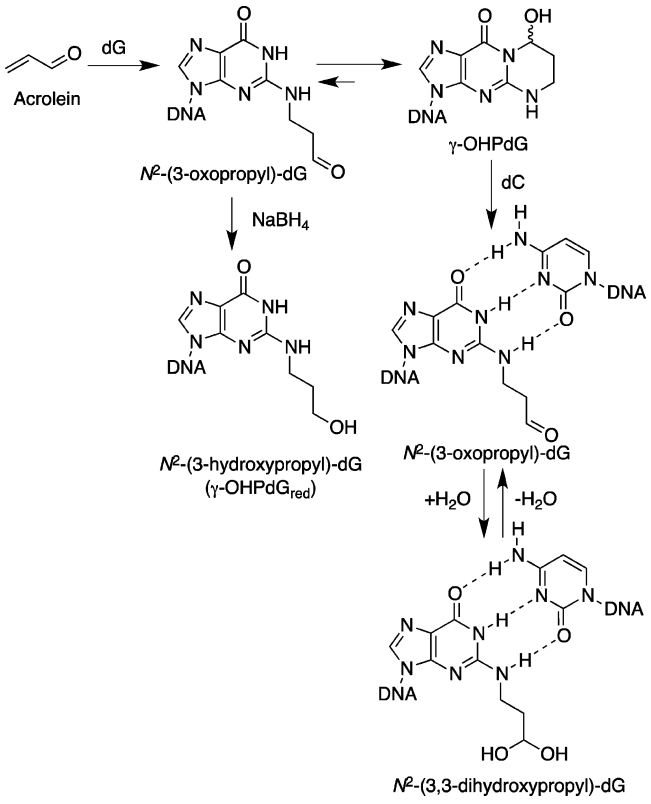

events were nonmutagenic in both *Escherichia coli* (≥99%)[21−23] and mammalian cells (≥89%).[23−27] These data were consistent with a model in which the nonmutagenic bypass of γ-OH-PdG was favored by adduct ring-opening.[15,23] Specifically, mutations were more frequently detected when single-stranded vectors were used with base substitutions, predominantly G to T transversions, occurring in various mammalian cell lines at frequencies from ∼4 to 11%.[23,26,27] When engineered into double-stranded vectors, the adduct was minimally mutagenic.[24,25] In contrast to γ-OH-PdG, the permanently ring-closed PdG adduct caused comparable mutation frequencies (ranging from ∼6 to 8%), regardless of whether single- or double-stranded vectors were utilized.[24,25,28] The N^2-(3-hydroxypropyl)-dG adduct (Scheme 1), an irreversibly ring-opened reduced derivative of γ-OH-PdG, was only marginally miscoding in mammalian cells, even though a single-stranded vector was used.[27]

In order to further understand the low mutagenicity of the γ-OH-PdG adduct, biochemical studies have been conducted with purified DNA polymerases and DNA templates containing γ-OH-PdG, reduced γ-OH-PdG (N^2-(3-hydroxypropyl)-dG, γ-OH-PdG$_{red}$), or PdG (reviewed in ref 29). Several members of the Y family of DNA polymerases have been identified that could bypass the γ-OH-PdG adduct. Yeast and human pol η,[26] human pol κ,[30] and *E. coli* pol IV (DinB)[31] manifested several common features, including inefficient nucleotide insertion opposite γ-OH-PdG, efficient insertion of the correct dC opposite γ-OH-PdG$_{red}$, and efficient primer extension from a dC placed opposite either γ-OH-PdG or γ-OH-PdG$_{red}$. When tested on the PdG-containing templates, pol η and pol κ failed to carry out extension.[26,32] Thus, it is inferred that the nonmutagenic replication bypass of γ-OH-PdG by pol η, pol κ, or pol IV is facilitated by a structural rearrangement of the adduct into its ring-opened structure.

The archebacterial DNA polymerase IV from *Sulfolobus solfataricus* P2 (Dpo4), a homologue of *E. coli* pol IV, is regarded as the prototypical Y-family polymerase. Dpo4 polymerase provides an excellent model for investigating the structural features that determine lesion bypass efficiency and fidelity.[33−41] Previously, the structures of several ternary Dpo4·DNA·dNTP complexes were determined with templates containing the PdG adduct.[36] In these complexes, the adduct remained in the *anti* conformation about the glycosyl bond, while the incoming dNTP skipped the modified template to form a Watson−Crick pair with the 5′-neighboring template nucleotide. Thus, ternary Dpo4·DNA·dNTP complexes with PdG in the polymerase active site were of the type II structure, according the nomenclature of Ling et al.[34]

In the present work, Dpo4 polymerase has been used to elucidate the structure of the γ-OH-PdG adduct during replication. We characterized Dpo4-catalyzed bypass of the γ-OH-PdG adduct and determined the structures of ternary Dpo4·DNA·dNTP complexes with γ-OH-PdG-containing templates.

MATERIALS AND METHODS

Materials. Dpo4 polymerase was expressed in *E. coli* and purified using heat denaturation, Ni^{2+}-nitriloacetate chromatography, and ion-exchange chromatography as described previously.[35] dNTPs were obtained from Amersham Biosciences (Piscataway, NJ). Oligodeoxynucleotides that were used as primers for preparation of the ternary Dpo4·DNA·dNTP complexes and all unmodified template oligodeoxynucleotides were obtained from Midland Certified Reagents (Midland, TX). Unmodified oligodeoxynucleotides that served as primers for *in vitro* replication assays were prepared by Molecular Microbiology and Immunology Research Core Facility of Oregon Health & Science University. All unmodified oligodeoxynucleotides were purified by anion-exchange chromatography by the suppliers. The biotinylated deoxyuridine(dU)-containing primer used for LC-ESI-MS-MS-based sequencing analyses was obtained from Midland Certified Reagents and tested for purity by capillary zone electrophoresis. The purity was greater than 99%.

Preparation of Adduct-Containing Oligodeoxynucleotides. The γ-OH-PdG adduct was synthesized, purified, and incorporated into template oligodeoxynucleotides using an established methodology.[42] The γ-OH-PdG$_{red}$ adduct was prepared by sodium borohydride reduction as described previously.[26] The modified oligodeoxynucleotides were characterized by MALDI-TOF mass spectrometry. The purity was assessed by capillary gel electrophoresis and C-18 HPLC methods. Oligodeoxynucleotide concentrations were determined by UV absorption at 260 nm.[43]

Replication Bypass Assays. The sequences of the template DNAs were 5′-TCACXGAATCCTTACGAGCCCCC-3′ and 5′-TCATXGAATCCTTACGAGCCCCC-3′, where X was dG, γ-OH-PdG, or γ-OH-PdG$_{red}$. Three different types of assays were conducted: primer extensions, single nucleotide incorporations, and primer extensions followed by LC-ESI-MS-MS sequencing.

The 18-mer oligodeoxynucleotide 5′-AAGGGGGCTCGT-AAGGAT-3′ served as the -3 primer in the primer extension reactions. The primer was ^{32}P-end-labeled and hybridized with the template 23-mer oligodeoxynucleotides according to the previously published procedures.[26] Dpo4-catalyzed reactions were carried out using 5 nM primer−template DNA substrates in the presence of 25 mM Tris-HCl (pH 7.5), 8 mM $MgCl_2$, 10% (v/v) glycerol, 5 mM NaCl, 0.1 mg/mL bovine serum albumin, 5 mM dithiothreitol, and 100 μM of each dNTP. Dpo4 concentrations ranged from 0.125 nM to 2 nM. The reactions were incubated for 10 min at 37 °C and terminated by the addition of an equal volume of a denaturing solution (95% (v/v)

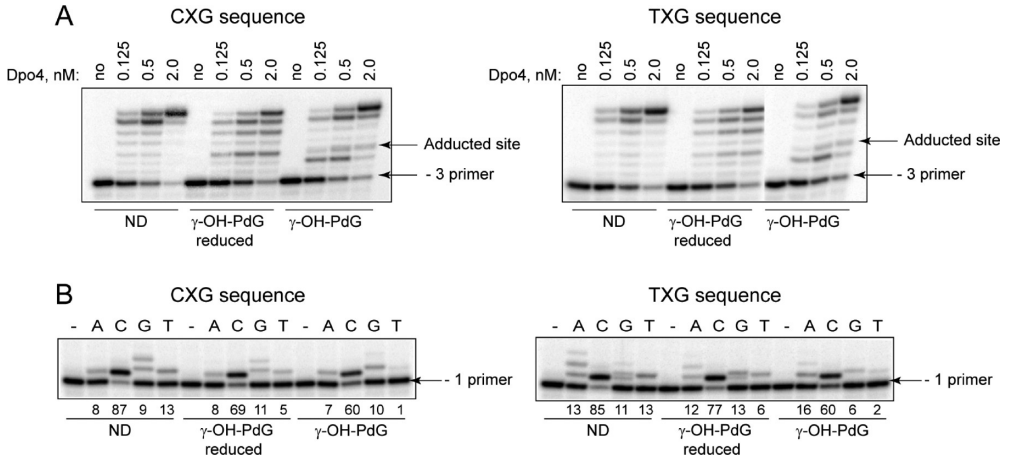

Figure 1. Replication bypass of the γ-OH-PdG and γ-OH-PdG$_{red}$ adducts by Dpo4. (A) Primer extensions by Dpo4 were carried out for 10 min at 37 °C in the presence of 100 μM dNTPs. (B) Single nucleotide incorporations opposite dG, γ-OH-PdG, or γ-OH-PdG$_{red}$ were carried out for 10 min at 37 °C in the presence of 1 nM Dpo4 and 20 μM individual dNTPs. The numbers below gel images represent the percentage of extended primers. ND, nondamaged template.

formamide, 20 mM Na_2EDTA, 0.2% (w/v) bromphenol blue, and 0.2% (w/v) xylene cyanol) followed by incubation at 95 °C for 2 min. The products were resolved through a 15% polyacrylamide gel containing 8 M urea. Following electrophoresis, the ^{32}P-labled DNAs were visualized using a PhosphorImager screen (GE Healthcare).

The 18-mer oligodeoxynucleotide 5′-GGGGGCTCGTAA-GGATTC-3′ was used in the single nucleotide incorporation assays as the -1 primer. Preparation of the primer−template DNA substrates, Dpo4-catalyzed reactions, and the product analyses were performed as described above, except that reactions contained 20 μM dNTP individually and that the Dpo4 concentration was 1 nM.

To generate bypass products for the LC-ESI-MS-MS sequencing analyses, the biotinylated dU-containing primer 5′-biotin-$(T)_{10}$-GGGGGCTCGTAAGGAUTC-3′ was hybridized with the template oligodeoxynucleotides and extended under conditions described above with the following modifications: DNA substrates (1.74 nmols) were incubated for 6 h in the presence of 100 nM Dpo4 and 1 mM of each dNTP; the total volume of the reaction was 200 μL. The cleavage of bypass products by *E. coli* uracil DNA glycosylase followed by piperidine treatment, purification of the piperidine cleavage fraction, and the LC-ESI-MS-MS sequencing were performed as previously described[38] with the following modifications. Final samples were dissolved in water (80 μL), and aliquots (8 μL) were injected with an autosampler. Mass spectrometric analyses were performed on a Waters Acquity UPLC system (Waters, Milford, MA) connected to a Finnigan LTQ mass spectrometer (ThermoElectron) that was equipped with an Ion Max API source and a standard electrospray probe using an Acquity UPLC BEH C18 column (1 μm, 1.0 mm × 100 mm). Product ion spectra were acquired over the range of m/z 345−2000. The ions were selected for collision-induced dissociation analyses, and the elucidation of the CID fragmentations of the candidate oligodeoxynucleotide sequence was done with the aid of Mongo Oligo Mass Calculator (v. 2.6, http://rna-mdb.cas.albany.edu/RNAmods/rnamass.htm). The quantification of the products was based on the ratio of the area peaks. The area peaks were calculated in the full scan mode of the extracted [M − 2H] and [M − 3H] ions for the analyte.

Crystallization of Ternary Dpo4·DNA·dNTP Complexes. Dpo4 polymerase was concentrated to 50−60 mg/mL using a spin concentrator with a 10^4M_r Amicon cutoff filter (Millipore, Inc., Billerica, MA) in 50 mM Tris-HCl buffer (pH 7.4 at 25 °C) containing 100 mM NaCl, 5 mM β-mercaptoethanol, and 50% glycerol (v/v). The 18-mer template oligodeoxynucleotides 5′-TCATXGAATCCT-TCCCCC-3′ and 5′-TCACXGAATCCTTCCCCC-3′, where X is the γ-OH-PdG adduct, were mixed with the 13-mer 5′-GGGGGAA-GGATTC-3′ or 14-mer 5′-GGGGGAAGGATTCC-3′ primer oligodeoxynucleotides at the 1:1 molar ratio in water. Dpo4 polymerase was combined with template/primer DNA at the 1:1.2 molar ratio, and the mixture was placed on ice for 30 min prior to incubation with 1 mM dNTP and 5 mM $CaCl_2$. Crystals were grown using the sitting drop vapor diffusion method by mixing 1 μL of complex with 1 μL of solution containing 50 mM Tris-HCl (pH 7.4 at 25 °C), 12−20% polyethylene glycol 3350 (w/v), 100 mM calcium diacetate, and 2.5% glycerol (v/v). Crystals were soaked in mother liquor containing an additional 25% polyethylene glycol 3350 (w/v) and 15% ethylene glycol (v/v) and flash-frozen in a stream of liquid nitrogen.

X-ray Diffraction Data Collection and Processing. Diffraction data sets for ternary complexes were collected at 100 K using a synchrotron radiation wavelength of 1.0 Å on the 21-ID-F beamline (Life Science Collaborative Access Team, LS-CAT) at the Advanced Photon Source (Argonne, IL). Indexing and scaling were performed using HKL2000.[44] The data were processed using CCP4 package programs,[45] and the truncate procedure was performed with TRUNCATE.[46]

Structure Determination and Refinement. The complex of Dpo4 polymerase with the 1,N^2-etheno-dG lesion[35] (downloaded from Protein Data Bank, with PDB code 2BQU) was used as a starting model. Following the removal of water molecules, modification of the template and primer sequences, and insertion of the γ-OH-PdG adduct, the cross-rotation and cross-translation functions were used to align the model with the experimental data. In each instance, several rounds of rigid body refinement of the diffraction data, with gradually increasing resolution, optimized the initial positions of the models. The models were refined further using CNS Solve (version 1.1),[47] by simulated annealing, gradient minimization, individual occupancy, and refinement of the individual isotropic temperature factors. Manual model building was performed using TURBO-FRODO.[48,49] A total of 5−10% of the reflections were excluded from the refinement to calculate the cross-validation residual R_{free}. Water oxygen atoms were added into positive regions (more than 3.0 standard deviations) of $F_o - F_c$ Fourier difference electron density during the manual model rebuilding steps. The crystallographic figures were prepared using PyMOL.[50]

Data Deposition. The results of the crystallographic analyses were deposited in the Protein Data Bank. The PDB identification numbers are 4JUZ (ternary complex of γ-OH-PdG-adducted DNA (0 primer) with Dpo4 and incoming dGTP), 4JV0 (ternary complex of γ-OH-PdG-adducted DNA (0 primer) with Dpo4 and incoming dATP), 4JV1 (ternary complex of γ-OH-PdG-adducted DNA (−1 primer) with Dpo4 and incoming dGTP), and 4JV2 (ternary complex of γ-OH-PdG-adducted DNA (−1 primer) with Dpo4 and incoming dATP).

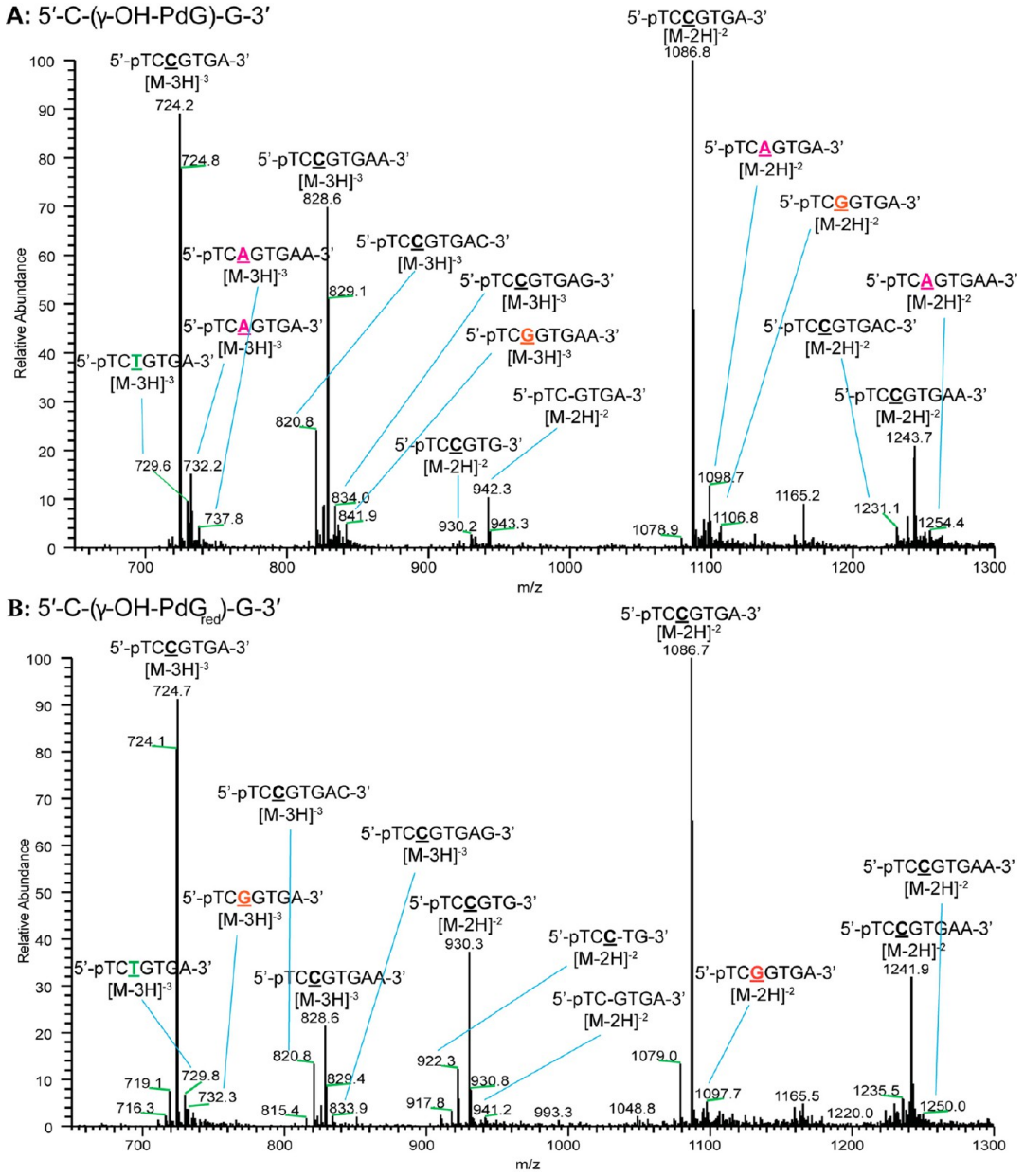

Figure 2. Full scan MS spectra of products obtained following replication past the γ-OH-PdG (A) and γ-OH-PdG$_{red}$ (B) adducts placed in the 5′-CXG-3′ sequence context.

RESULTS

Replication Bypass of γ-OH-PdG by the Dpo4 Polymerase. To test for the ability of Dpo4 to replicate past the γ-OH-PdG adduct or its irreversibly ring-opened analogue, γ-OH-PdG$_{red}$, Dpo4-catalyzed reactions were conducted in the presence of all four dNTPs. The primer was designed such that following annealing to the template DNAs, its 3′ end would be positioned three nucleotides upstream of the modified site (−3 primer). The template sequences were designed to contain the lesion in either the 5′-CXG-3′ or the 5′-TXG-3′ sequence. The control reactions were conducted with the two corresponding nondamaged primer−template DNAs. As expected, the Dpo4 polymerase extended the primers to full length products on nondamaged substrates in a concentration-dependent manner (Figure 1A). However, a pause site was observed opposite the lesion when similar reactions were conducted with DNAs containing the γ-OH-PdG$_{red}$ adduct in both sequence contexts. Accumulation of the extension products was also detected at the +2 position relative to the lesion site, suggesting that γ-OH-PdG$_{red}$ may impede the reaction two nucleotides downstream of the lesion. With the γ-OH-PdG-adducted templates, the extent of the blockage to DNA synthesis was more severe, with a major pause site detected one nucleotide prior to the lesion and another pause site opposite the lesion.

Single nucleotide incorporation experiments were conducted to determine the identities of nucleotides inserted opposite the γ-OH-PdG and γ-OH-PdG$_{red}$ adducts by the Dpo4 polymerase. In all of the cases, the primers were most efficiently extended in the presence of dCTP, regardless of the sequence context or the template nucleotide (Figure 1B). Consistent with the results of the primer extension experiments (Figure 1A), the percentage of primers extended in the presence of dCTP was highest (87 ± 1) on the nondamaged templates, intermediate (75 ± 6) on the γ-OH-PdG$_{red}$-containing templates, and lowest

dx.doi.org/10.1021/tx400200b | Chem. Res. Toxicol. 2013, 26, 1348−1360

Table 1. Products of Dpo4-Catalyzed Bypass of the γ-OH-PdG and γ-HO-PdG$_{red}$ Adducts in the 5′-CXG-3′ and 5′-TXG-3′ Sequence Contexts[a]

extension product	γ-OH-PdG	γ-OH-PdG$_{red}$	comment
3′--AGXCACT-5′ (5′-CXG-3′ template)			
5′-pTCCGTGA-3′ (m/z [M-3H]$^{-3}$ 724.1; [M-2H]$^{-2}$ 1086.7)	50%	68%	error-free
5′-pTCCGTGAA-3′ (m/z [M-3H]$^{-3}$ 828.5; [M-2H]$^{-2}$ 1243.2)	21%	7%	
5′-pTCCGTGAC-3′ (m/z [M-3H]$^{-3}$ 820.5; [M-2H]$^{-2}$ 1231.2)	3%	4%	
5′-pTCCGTGAG-3′ (m/z [M-3H]$^{-3}$ 833.8)	3%	1%	
5′-pTCCGTG-3′ (m/z [M-2H]$^{-2}$ 930.1; [M-3H]$^{-3}$ 1251.2)	1%	11%	
5′-pTCAGTGA-3′ (m/z [M-3H]$^{-3}$ 732.1; [M-2H]$^{-2}$ 1098.7)	7%	2%	misinsertion of dA
5′-pTCAGTGAA-3′ (m/z [M-3H]$^{-3}$ 737.5; [M-2H]$^{-2}$ 1255.2)	1%		
5′-pTCGGTGA-3′ (m/z [M-2H]$^{-2}$ 1106.8)	2%		misinsertion of dG
5′-pTCGGTGAA-3′ (m/z [M-3H]$^{-3}$ 841.8; [M-2H]$^{-2}$ 1263.2)	1%		
5′-pTCTGTGA-3′ (m/z [M-3H]$^{-3}$ 729.1)	2%	3%	misinsertion of dT
5′-pTC−GTGA-3′ (m/z [M-2H]$^{-2}$ 942.2)	2%	1%	deletion
5′-pTCC−TGA-3′ (m/z [M-2H]$^{-3}$ 922.1)		2%	deletion
3′--AGXTACT-5′ (5′-TXG-3′ template)			
5′-pTCCATGA-3′ (m/z [M-3H]$^{-3}$ 718.8; [M-2H]$^{-2}$ 1078.7)	55%	28%	error-free
5′-pTCCATGAA-3′ (m/z [M-3H]$^{-3}$ 823.1; [M-2H]$^{-2}$ 1235.2)	15%	52%	
5′-pTCCATGAC-3′ (m/z [M-3H]$^{-3}$ 815.1; [M-2H]$^{-2}$ 1243.2)	12%	8%	
5′-pTCCATGAG-3′ (m/z [M-3H]$^{-3}$ 828.5; [M-2H]$^{-2}$ 1223.2)	3%	1%	
5′-pTCCATG-3′ (m/z [M-2H]$^{-2}$ 922.1)	1%	3%	
5′-pTCAATGA-3′ (m/z [M-3H]$^{-3}$ 726.8; [M-2H]$^{-2}$ 1090.7)	3%		misinsertion of dA
5′-pTCGATGA-3′ (m/z [M-3H]$^{-3}$ 732.1; [M-2H]$^{-2}$ 1098.7)	4%	1%	misinsertion of dG
5′-pTCGATGAA-3′ (m/z [M-3H]$^{-3}$ 836.5; [M-2H]$^{-2}$ 1255.2)	1%		
5′-pTCTATGA-3′ (m/z [M-3H]$^{-3}$ 723.8; [M-2H]$^{-2}$ 1086.2)	5%	2%	misinsertion of dT
5′-pTC−ATGA-3′ (m/z [M-2H]$^{-2}$ 934.2)	1%		deletion

[a]The sum of the percentages is less than 100% since in addition to the listed products, some unidentified extension products were present as minor species.

(60 ± 2) on the γ-OH-PdG-containing templates (the data represent the mean values obtained from four independent experiments with standard deviations).

The extension products were also formed in all of the reactions containing incorrect dNTPs, even with the non-damaged templates. With the 5′-CXG-3′ templates, several sequential incorporation events occurred in the presence of dGTP. With the 5′-TXG-3′ templates, similar patterns were observed in the presence of dATP. Thus, when the incoming nucleotide was complementary to the 5′-neighboring template nucleotide, the replication could proceed via a series of the primer−template misalignments/realignments.

The above data showed a relatively accurate nucleotide insertion opposite both the γ-OH-PdG and γ-OH-PdG$_{red}$ adducts. However, since the mutagenic outcome of the overall bypass reactions can be modulated at the extension step, LC-ESI-MS-MS-based sequencing assays[38,51] were performed to further evaluate the fidelity of Dpo4-catalyzed replication past these lesions. Specifically, the 5′-biotinylated primer containing a dU near the primer−template junction was hybridized with the adducted templates and extended by the Dpo4 polymerase to generate bypass products. The primers were immobilized on streptavidin-coated polystyrene beads, washed, and cleaved at the dU sites by sequential treatment with uracil DNA glycosylase and piperidine. The 3′-terminal cleavage products were isolated and analyzed by LC-ESI-MS-MS. The mass spectrometric data are provided in Figures S1−S34 of the Supporting Information.

Full scan MS spectra for the extension of the γ-OH-PdG and γ-OH-PdG$_{red}$ adducts in the 5′-CXG-3′ templates are shown in Figure 2. The sequences of the extension products (Table 1) were determined by analyses of the CID spectra (Figures S9−S20 of the Supporting Information) as previously described.[38,51] The most abundant replication products for both adducts were derived for the correct insertion of dCTP, followed by error-free extension. These included the expected error-free product as well as those derived from the blunt end addition of dATP, dCTP, and dGTP; the incomplete extension of the primer was also observed. Misreplication products were observed in low abundance. These products included the misinsertion of dATP, dGTP, and dTTP opposite the γ-OH-PdG adduct, and misinsertion of dATP and dTTP opposite the γ-OH-PdG$_{red}$ adduct. Low levels of a one-nucleotide deletion product were observed for both adducts in this sequence; additionally, an unusual deletion product in which dCTP was inserted opposite the lesion followed by deletion of the next downstream nucleotide was identified for γ-OH-PdG$_{red}$ only.

The most abundant bypass products observed for both adducts in the 5′-TXG-3′ template were also derived from error-free replication (Figures S23−S34 of the Supporting Information). These included the expected error-free product, as well as those derived from blunt end additions of dATP, dCTP, and dGTP, and incomplete extension. Minor extension products were observed, which resulted from misinsertion of dATP, dGTP, and dTTP opposite the γ-OH-PdG adduct, while misinsertion of dGTP and dTTP were observed for the γ-OH-PdG$_{red}$ adduct. In addition, minor amounts of a one-nucleotide deletion product were observed for the γ-OH-PdG adduct, but not its reduced derivative.

The relative yields of the various extension products were estimated from the peak areas of the reconstructed LC-MS ion chromatograms (Figures S6−S8 and S21−S22 of the

Table 2. List of the Ternary Dpo4·DNA·dNTP Complexes Used for Crystallography[a]

Complex	DNA	Polymerase	dNTP
Complex **1**	3′- **C**CTTAGGAAGGGGG -5′ (14-mer) 5′- TCA**CXG**AATCCTTCCCCC -3′ (18-mer)	Dpo4	dGTP
Complex **2**	3′- **C**CTTAGGAAGGGGG -5′ (14-mer) 5′- TCA**TXG**AATCCTTCCCCC -3′ (18-mer)	Dpo4	dATP
Complex **3**	3′- CTTAGGAAGGGGG -5′ (13-mer) 5′- TCA**CXG**AATCCTTCCCCC -3′ (18-mer)	Dpo4	dGTP
Complex **4**	3′- CTTAGGAAGGGGG -5′ (13-mer) 5′- TCA**TXG**AATCCTTCCCCC -3′ (18-mer)	Dpo4	dATP

[a]Bold letters represent the modified site along with 5′- and 3′-neighbors.

Table 3. Crystallographic Data and Refinement Parameters for the Ternary Dpo4·DNA·dNTP Complexes Containing the γ-OH-PdG Adduct

	5′-CXG-3′	5′-TXG-3′	5′-CXG-3′	5′-TXG-3′
complex	**1**	**2**	**3**	**4**
X-ray source (beamline)	LS-CAT	LS-CAT	LS-CAT	LS-CAT
wavelength (Å)	0.978	0.978	0.978	0.978
temperature (K)	100	100	100	100
space group	$P2_12_12$	$P2_12_12$	$P2_12_12$	$P2_12_12$
unit cell (*a*, *b*, *c*; Å)	94.91, 104.36, 52.49	93.83, 104.49, 52.53	93.27, 102.18, 52.73	94.58, 103.31, 52.78
resolution range (Å)	50−2.65	50−2.9	50−2.3	50−2.75
highest resolution shell	2.74−2.65	3.0−2.9	2.38−2.3	2.85−2.75
no. of measurements	103702	74402	159237	94938
no. of unique reflections	15480	11170	23031	14000
redundancy	6.7 (3.7)	6.4 (3.5)	6.9 (5.0)	6.8 (4.4)
completeness (%)	98.8 (90.8)	97.7 (87.9)	99.0 (92.7)	99.4 (94.9)
R_{merge} (%)	7.3 (54.5)	12.4 (56.5)	5.9 (49.0)	8.8 (64.4)
signal-to-noise ($I/\sigma I$)	22.2 (2.3)	15.1 (2.7)	28.1 (2.3)	21.3 (2.1)
solvent content (%)	60.3	59.8	58.8	59.9
Model Composition (Asymmetric Unit)				
no. of amino acid residues	342	342	342	342
no. of water molecules	40	45	85	40
no. of Ca^{2+} ions	2	2	3	2
no. of template nucleotides	18	18	18	18
no. of primer nucleotides	14	14	13	13
no. of dGTPs	1		1	
no. of dATPs		1		1
R_f (%)	21.0	18.9	21.3	20.3
R_{free} (%)	27.3	26.0	26.9	26.6
Temperature Factors				
Wilson plot (Å^2)	60.1	70.3	52.7	60.5
bonded main chain atoms (Å^2)	55.4	69.7	50.8	54.9
bonded side chain atoms (Å^2)	59.6	74.2	55.0	58.3
rmsd from Ideal Values				
bond lengths (Å)	0.009	0.009	0.009	0.009
bond angles (deg)	1.3	1.3	1.2	1.3
dihedral angles (deg)	21.3	21.6	22.0	22.2

Supporting Information); the sum of the peak areas were used when both the $[M\text{-}2H]^{-2}$ and $[M\text{-}3H]^{-3}$ charge states of products were observed (Table 1). The MS data demonstrated that error-free bypass of the γ-OH-PdG and γ-OH-PdG$_{red}$ lesions was favored by Dpo4 polymerase in both sequence contexts. The error-free products, including the blunt end insertion and incomplete extension products, constituted ∼78% and 86% of the total extension products obtained, following replication past the γ-OH-PdG adduct in the 5′-CXG-3′ and 5′-TXG-3′ contexts, respectively. The γ-OH-PdG$_{red}$ adduct was bypassed more accurately with the error-free products representing ∼91% and 92% of the total extension products

dx.doi.org/10.1021/tx400200b | *Chem. Res. Toxicol.* 2013, 26, 1348−1360

in the 5′-CXG-3′ and 5′-TXG-3′ contexts, respectively. These data support the interpretation that the ring-opening favors error-free bypass of the adduct.

Regarding the misinsertion events that occurred during replication bypass of γ-OH-PdG, dA was most frequently present at the site opposite the lesion in the 5′-CXG-3′ sequence. With the 5′-TXG-3′ sequence, the LC-ESI-MS-MS analyses showed that misinsertion of dTTP and dGTP predominated, although the differences were small. Thus, misincorporations due to the base-pairing between an incoming dNTP and a 5′-neighboring template nucleotide were not the prevalent mechanism for generating base substitutions.

The data of the replication assays *in vitro* demonstrated that similar to pol *η*, pol *κ*, and pol IV,[26,30−32] Dpo4 polymerase was capable of replication past both γ-OH-PdG and γ-OH-PdG$_{red}$, preferentially inserting the correct nucleotide opposite these adducts and manifesting a higher tolerance for the latter adduct at the nucleotide insertion step. On the basis of these observations, we hypothesized that opposite dC, the ring-open conformation was preferred in the active site of Dpo4 polymerase and that the overall complex structure favored further primer extension; when a nucleotide was misincorporated due to base-pairing with the 5′ template nucleotide, nonproductive complexes were formed. In order to validate the proposed model, ternary Dpo4·DNA·dNTP complexes containing γ-OH-PdG-adducted templates were crystallized and analyzed.

Crystallization of Ternary Dpo4·DNA·dNTP Complexes. To obtain ternary Dpo4·DNA·dNTP complexes, γ-OH-PdG was site-specifically incorporated into two 18-mer templates in which the adduct was either in the 5′-CXG-3′ or 5′-TXG-3′ sequence context. The primers were designed such that the 3′ end would be positioned one nucleotide upstream of γ-OH-PdG (−1 primer) or would have a dC opposite the adduct (0 primer). Crystallization trials were conducted with various primer−template combinations, Dpo4, each of the four dNTPs, and Ca^{2+}, an inhibitor of DNA polymerases. Although the structure of the complex containing incoming dCTP opposite the γ-OH-PdG adduct was of interest, the crystals obtained from those complexes yielded poor diffraction data. Thus, the present study focuses on the structures of complexes **1**−**4** (Table 2), which showed single crystals with good diffraction data. With the 5′-CXG-3′ template annealed with either the 0 or −1 primer, Dpo4 polymerase cocrystallized in the presence of dGTP and $CaCl_2$ (complexes **1** and **3**, respectively). With the 5′-TXG-3′ template annealed with either the 0 or −1 primer, Dpo4 cocrystallized in the presence of dATP and $CaCl_2$ (complexes **2** and **4**, respectively). All of the complexes crystallized in the orthorhombic crystal system in the space group $P2_12_12$. The crystals diffracted X-rays to resolutions between 2.3 and 2.9 Å. The overall completeness and redundancy of reflections were of sufficient quality for model building. Details of data collection, data processing, and data quality for these ternary complexes are summarized in Table 3.

Ring-Opening of the γ-OH-PdG Adduct When Placed Complementary to dC at the Primer−Template Junction (complexes 1 and 2). The structure of the ternary Dpo4·DNA·dGTP complex **1** involving the 5′-CXG-3′ template was determined at 2.65 Å. In this complex, the γ-OH-PdG adduct was positioned complementary to dC at the 3′ primer terminus (Table 2). The active site of Dpo4 polymerase is shown in Figure 3A. Confirming our hypothesis, the γ-OH-PdG adduct

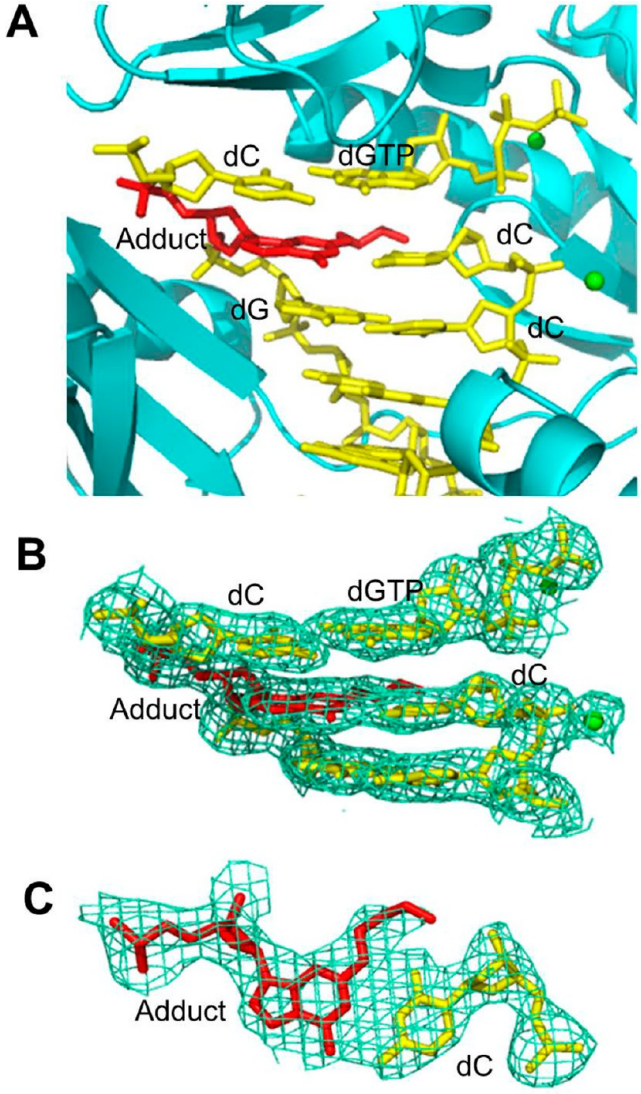

Figure 3. Structure of the ternary Dpo4·DNA·dGTP complex **1**. (A) Active site of Dpo4 (cartoon form, cyan) containing a primer−template junction (yellow) with the ring-opened N^2-(3-oxopropyl)-dG or N^2-(3,3-dihydroxypropyl)-dG adduct (red) opposite the 3′-terminal dC, incoming dGTP (yellow), and Ca^{2+} ions (green dot). (B) Electron density at the active site. (C) Top view of the Watson−Crick base pair between the adduct and the 3′-terminal dC. All electron densities are from $(2F_o - F_c)$ maps at the 1σ level.

was present in its ring-opened form opposite the 3′-terminal dC (0 primer) in the Dpo4 active site. The template dC that is the 5′-neighbor of the adducted dG, and the incoming dGTP were also accommodated within the active site. The modified dG, its complementary dC, and the incoming dGTP exhibited strong electron density (Figure 3B). However, the electron density around the terminus of the open alkyl chain was poorly defined (Figure 3C), presumably because the ring-opened adduct could be either N^2-(3-oxopropyl)-dG or N^2-(3,3-dihydroxypropyl)-dG (Scheme 1). The modified base adopted the *anti* conformation and was stacked inside the duplex, while the alkyl chain pointed toward the minor groove. The ring-opening exposed the Watson−Crick face of the damaged dG, allowing Watson−Crick hydrogen bonding with dC at the primer terminus. The incoming dGTP was positioned opposite the 5′-neighboring template dC to facilitate the formation of a

dx.doi.org/10.1021/tx400200b | *Chem. Res. Toxicol.* 2013, 26, 1348−1360

Watson−Crick pair. The distance between the primer 3′-hydroxyl and the α-phosphate of the incoming dGTP was 4.8 Å. To avoid model bias, a simulated annealing omit map was calculated at the adducted and complementary nucleotides. Further, the map was calculated for the ring-closed γ-OH-PdG adduct and also for *anti* and *syn* orientations of the modified base. The positive $F_o - F_c$ map confirmed the ring-opening of γ-OH-PdG and the *anti* conformation. The 5′-terminal template nucleotide was disordered, and three nucleotides located 5′ to the adduct displayed elevated thermal parameters. Two Ca^{2+} ions were identified in this structure, one in the active site and another in the thumb region (Figure 3).

The structure of the ternary Dpo4·DNA·dATP complex **2** involving the 5′-TXG-3′ template was determined at 2.9 Å. Similar to the structure involving the 5′-CXG-3′ template, the γ-OH-PdG adduct was present in its ring-opened form, and the Watson−Crick face of the adduced base was exposed toward the complementary dC at the 3′ terminus of the primer (Figure 4A). The ring-opened γ-OH-PdG, its complementary dC, and the incoming dATP were surrounded by strong electron density (Figure 4B). Consistent with the previous structure (complex **1**), the electron density around the terminus of the open alkyl chain was weak (Figure 4C), suggesting that the adduct could be either the aldehyde or its hydrate. Also similar to complex **1**, the adducted base was in the *anti* conformation and stacked inside the duplex, while the alkyl chain was oriented toward the minor groove. The incoming dATP was positioned to form Watson−Crick hydrogen bonding with the 5′-neighboring template dT. As in the case of the 5′-CXG-3′ template, the alternative maps were calculated to confirm the ring-opening of γ-OH-PdG and the *anti* conformation of the adducted base. The 5′-end of the template was disordered, and three nucleotides on the 5′ side of the adduct displayed elevated thermal parameters. The distance between the primer 3′-hydroxyl and the α-phosphate of the incoming dGTP was 4.2 Å in this structure. Two Ca^{2+} ions were identified, and the positions of these ions were close to their positions in complex **1**. Superposition of the structures of complexes **1** and **2** (Figure 5) demonstrated a high degree of similarity, suggesting that the mechanism of Dpo4-catalyzed primer extension from dC opposite the γ-OH-PdG adduct was independent of the identity of the template pyrimidine nucleotide.

Formation of the Type-II Structure of γ-OH-PdG in the Absence of Complementary dC at the Primer−Template Junction (complexes 3 and 4). The structure of the ternary Dpo4·DNA·dGTP complex **3** with the 5′-CXG-3′ template was determined at 2.3 Å resolution. Figure 6A shows the active site of Dpo4 polymerase in which the γ-OH-PdG adduct, its 5′-neighboring template dC, and the incoming dGTP were accommodated. The overall structure resembles the type II structure that was observed for Dpo4 cocrystallized with native DNA.[34] In complex **3**, γ-OH-PdG remained in the ring-closed form (Figure 6A and B). The adducted base was in the *anti* conformation and stacked inside the duplex. The exocyclic ring precluded correct positioning of the incoming dGTP. Instead, dGTP skipped the adducted nucleotide to form a Watson−Crick pair with the 5′-neighboring template dC, while the 3′-terminal primer dC was properly paired with the 3′-neighboring template dG. A top view of electronic density around the DNA helical axis at the 5′-neighboring template dC and the incoming dGTP confirmed the positions and the conservation of Watson−Crick hydrogen bonding (Figure 6C). The 3′-hydroxyl of the primer and the α-phosphate of the incoming dGTP were 5.7 Å apart, a value that exceeds the optimal distance for catalysis. Similar to the type II structure of native DNA,[34] three Ca^{2+} ions were identified.

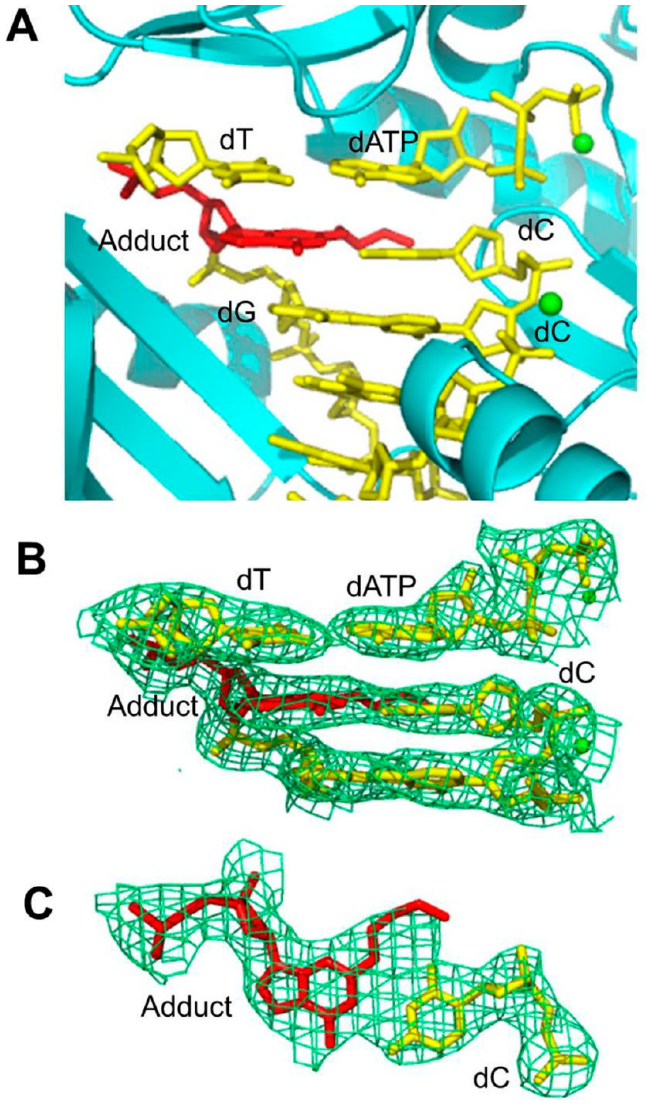

Figure 4. Structure of the ternary Dpo4·DNA·dATP complex **2**. (A) Active site of Dpo4 (cartoon form, cyan) containing a primer/template junction (yellow) with the ring-opened N^2-(3-oxopropyl)-dG or N^2-(3,3-dihydroxypropyl)-dG adduct (red) opposite the 3′-terminal dC, incoming dATP (yellow), and Ca^{2+} ions (green dot). (B) Electron density at the active site. (C) Top view of the Watson−Crick base pair between the adduct and the 3′-terminal dC. All electron densities are from $(2F_o - F_c)$ maps at the 1σ level.

The structure of the ternary Dpo4·DNA·dATP complex **4** involving the 5′-TXG-3′ template was determined at 2.75 Å resolution. Similar to complex **3**, the polymerase active site resembled the type II structure (Figure 7A and B). The γ-OH-PdG adduct remained in its ring-closed form. The 5′-neighboring template dT and the incoming dATP were paired, utilizing the Watson−Crick geometry (Figure 7C). This resulted in a gap of 6.6 Å between the 3′-hydroxyl of the primer and the α-phosphate of the dATP, which was even larger than the corresponding distance in complex **3**. The 5′-end template nucleotide was disordered, and three bases on that side of the adduct had elevated thermal parameters. Although the active site structure of the Dpo4 polymerase

dx.doi.org/10.1021/tx400200b | *Chem. Res. Toxicol.* 2013, 26, 1348−1360

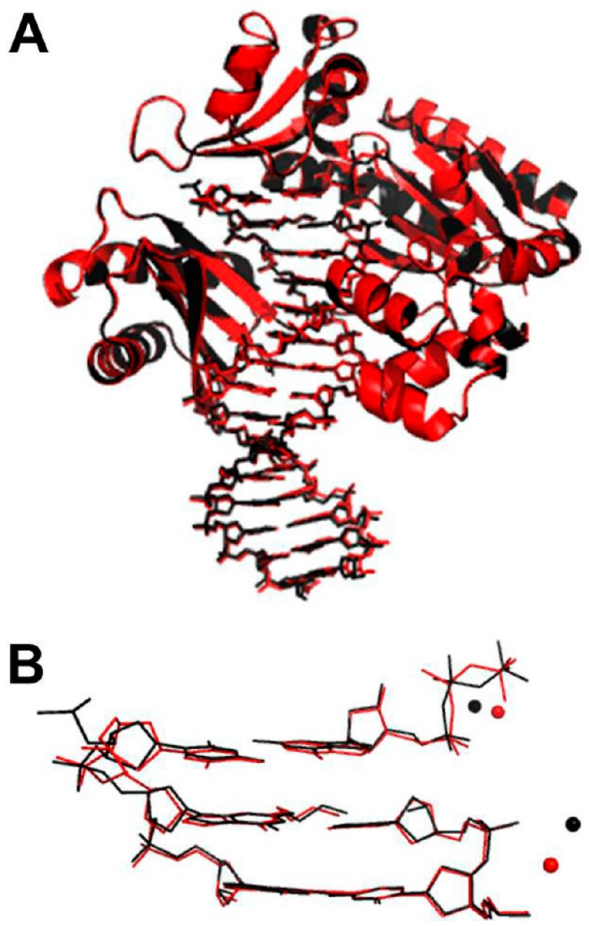

Figure 5. Superimposed structures of the ternary Dpo4·DNA·dNTP complexes **1** and **2**. Overall conformations (A) and modified DNA conformations and positions of Ca^{2+} ions (B) at the active site. Complexes **1** and **2** are colored in black and red, respectively. (RMSD = 0.315 Å).

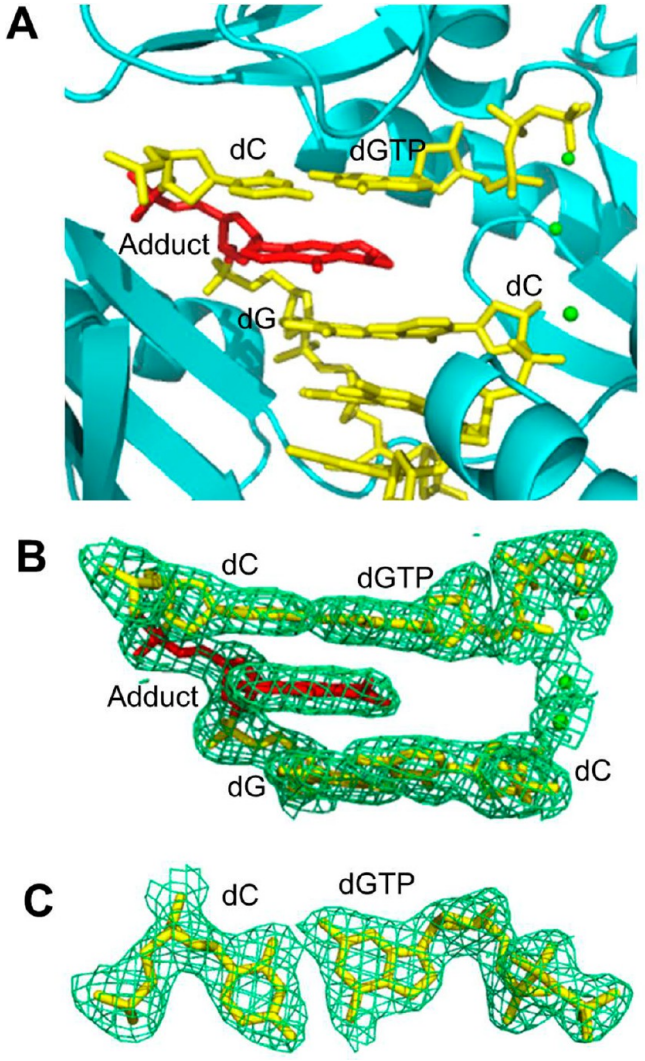

Figure 6. Structure of the ternary Dpo4·DNA·dGTP complex **3**. (A) Active site of Dpo4 (cartoon form, cyan) containing a primer–template junction (yellow) with the ring-closed γ-OH-PdG adduct (red), incoming dGTP (yellow), and Ca^{2+} ions (green dot). (B) Electron density at the active site. (C) Top view of the Watson–Crick base pair between incoming dGTP and the 5′-neighboring template dC. All electron densities are from $(2F_o - F_c)$ maps at the 1σ level.

resembled the type II structure, only two bound Ca^{2+} ions were identified at the current resolution level. Superimposition of complex **3** and complex **4** (Figure 8) demonstrated only subtle differences between these structures. With both templates, the adduct remained ring-closed, incoming nucleotides formed a Watson–Crick pair with the complementary 5′ template nucleotides, and the overall active site structures deviated from the catalytically competent conformation.

DISCUSSION

Replication of DNA containing the major acrolein-induced lesion, γ-OH-PdG, represents a formidable challenge for the DNA-synthesizing machinery. The adduct has been shown to be a severe block and a miscoding lesion for a number of the high-fidelity DNA polymerases, including the major mammalian replicative polymerases, pol δ and pol ε.[21−23,32] Thus, the efficient and relatively accurate bypass of γ-OH-PdG that has been observed in both bacterial and mammalian experimental systems[21−27] must be provided by DNA polymerases specifically adapted for translesion DNA synthesis.

Prior studies have demonstrated that the Y-family DNA polymerases, yeast and human pol η,[26] human pol κ,[30,32] and *E. coli* pol IV,[27] can synthesize DNA past γ-OH-PdG. Although these polymerases are partially blocked by γ-OH-PdG one nucleotide before the lesion, they preferentially incorporate the correct dCTP opposite to that site and efficiently extend the primers. Conversion of the adduct to the permanently ring-opened, reduced derivative prior to replication results in a significant increase in the correct nucleotide insertion but has no appreciable effect on extension.[26,27,32] In contrast, the ring-closed PdG adduct is a strong block for both sequential steps of the bypass reaction.[26,32] The present study shows that Dpo4 is able to replicate past γ-OH-PdG by preferentially incorporating the correct dCTP opposite the lesion and carrying out the subsequent primer extension. Relative to γ-OH-PdG, γ-OH-PdG_{red} is notably less inhibiting to Dpo4-catalyzed dCTP insertion opposite the lesion site and causes fewer replication errors. Thus, we hypothesized that the error-free replication bypass of γ-OH-PdG by the Dpo4 polymerase requires the adduct to be in its ring-opened form, as has been proposed for pol η, pol κ, and pol IV.

In order to provide structural evidence for this hypothesis, we solved the crystal structures of ternary Dpo4·DNA·dNTP

dx.doi.org/10.1021/tx400200b | *Chem. Res. Toxicol.* 2013, 26, 1348−1360

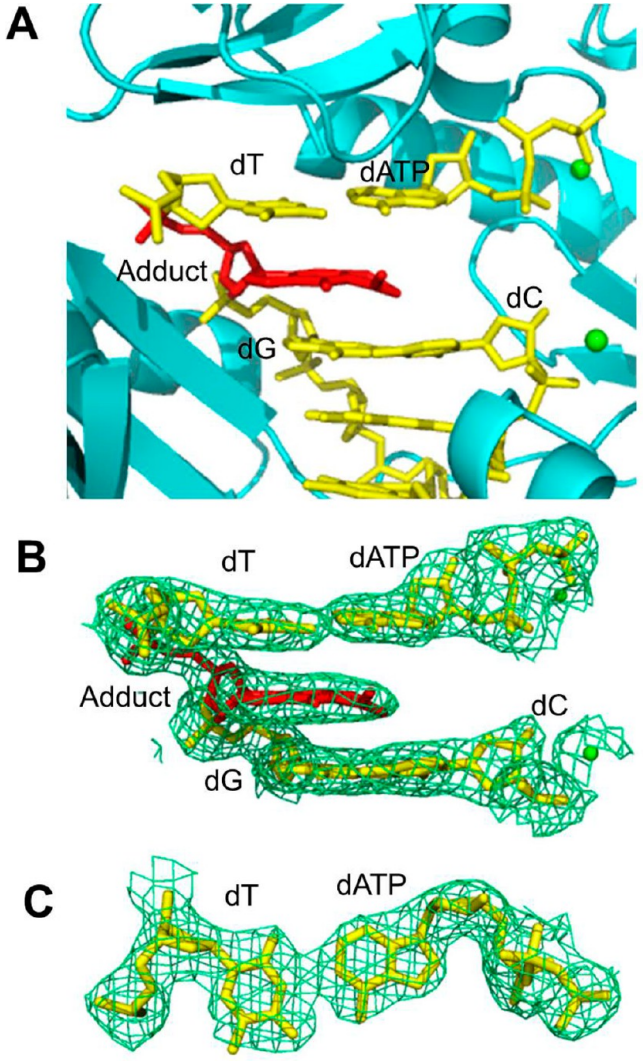

Figure 7. Structure of the ternary Dpo4·DNA·dATP complex **4**. (A) Active site of Dpo4 (cartoon form, cyan) containing a primer–template junction (yellow) with the ring closed γ-OH-PdG adduct (red), incoming dATP (yellow), and Ca^{2+} ions (green dot). (B) Electron density at the active site. (C) Top view of the Watson–Crick base pair between incoming dATP and the 5′-neighboring template dT. All electron densities are from $(2F_o - F_c)$ maps at the 1σ level.

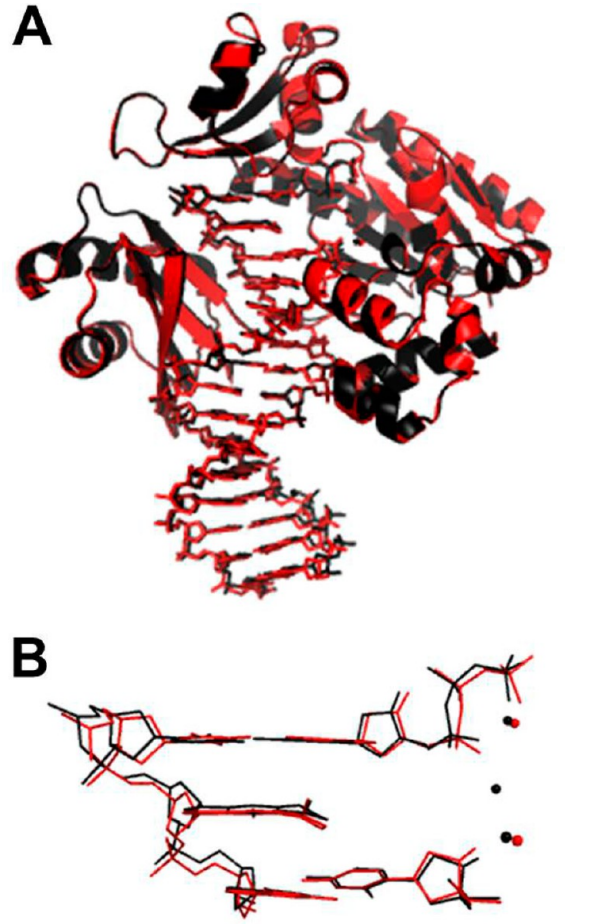

Figure 8. Superimposed structures of the ternary Dpo4·DNA·dNTP complexes **3** and **4**. Overall conformations (A) and modified DNA conformations and positions of Ca^{2+} ions (B) at the active site. Complexes **3** and **4** are colored in black and red, respectively. (RMSD = 0.309 Å).

complexes that involved γ-OH-PdG-containing templates. Specifically, γ-OH-PdG was placed opposite dC at the primer–template junction, and the incoming dNTP was provided to complement the template nucleotide, 5′ adjacent to the modified nucleotide (dGTP with the 5′-CXG-3′ template (complex **1**) and dATP with the 5′-TXG-3′ template (complex **2**)). These structures represent models of bypass intermediates that could be generated following the insertion of dCTP opposite the lesion but prior to formation of the next phosphodiester bond. The analyses of the ternary complexes **1** and **2** illustrate that at the active site of the Dpo4 polymerase, γ-OH-PdG exists in the ring-opened conformation, assumes the *anti* orientation about the glycosyl bond, and pairs with the opposing dC using the Watson–Crick geometry. These data constitute evidence that γ-OH-PdG can undergo ring-opening opposite dC not only in double-stranded DNA[15–17] but also at the primer–template junction in the active site of this polymerase.

Ternary complex **1** shows the incoming dGTP opposite template dC. Ternary complex **2** shows the incoming dATP opposite template dT. In both cases, the incoming dNTP is properly stacked and hydrogen bonded to the template nucleotide, while the primer 3′-hydroxyl is positioned to facilitate catalysis. The overall DNA structure in both ternary complexes remains stabilized by Watson–Crick and stacking interactions. Thus, the Dpo4 polymerase can accommodate the ring-opened form of γ-OH-PdG opposite dC in the active site to satisfy the geometry of the catalytically competent replication intermediate. This observation is significant since it explains how Y family DNA polymerases can diminish the blocking and mutagenic potential of the γ-OH-PdG lesion.

In addition to γ-OH-PdG, other exocyclic dG adducts that are capable of ring-opening opposite dC in DNA have been identified. These include the malondialdehyde-induced lesion 3-(2′-deoxy-β-D-*erythro*-pentofuranosyl)pyrimido[1,2-*a*]purin-10(3*H*)-one (M_1dG)[52] and stereoisomers of the crotonaldehyde- and *trans*-4-hydroxynonenal-1,N^2-dG adducts.[53–55] Ring-opening at the primer–template junction opposite dC has previously been observed for the (6*S*,8*R*,11*S*)-hydroxynonenal-1,N^2-dG adduct in the active site of the Dpo4 polymerase.[41] In contrast, M_1dG remained ring-closed opposite dC in the Dpo4·DNA·dNTP postinsertion complex.[37] The authors hypothesized that either the Dpo4 active site is not restrictive enough to

dx.doi.org/10.1021/tx400200b | *Chem. Res. Toxicol.* 2013, 26, 1348–1360

force dC to stabilize M_1dG ring-opening or that the level of dC hydration is reduced in the active site of the polymerase relative to DNA in solution. In contrast to γ-OH-PdG, the ring-opening of M_1dG requires hydration at the N3 atom of dC.

The LC-ESI-MS-MS-based sequencing analyses of full-length bypass products demonstrates that although the Dpo4 polymerase can replicate past the γ-OH-PdG and γ-OH-PdG_{red} adducts accurately, misinsertions and one nucleotide deletions are detected opposite the lesion sites. Misinsertion of dATP opposite γ-OH-PdG is a predominant error in the 5′-CXG-3′ sequence context. Importantly, this matches the spectra of γ-OH-PdG-induced mutations that have been observed following intracellular replication of vectors containing the adduct in the 5′-CX-3′ sequences.[23−27] In the 5′-TXG-3′ sequence context, misinsertions of dGTP and dTTP are more common. The mechanisms responsible for misinsertions of dATP in the 5′-CXG-3′ context and either dGTP or dTTP in the 5′-TXG-3′ context have not been addressed in the present study. However, NMR spectroscopic analyses have been performed, in which γ-OH-PdG was positioned in the 5′-CXA-3′ sequence opposite either dA or dT in otherwise complementary strands.[17] Opposite dA, the adduct predominantly existed in its ring-closed conformation, suggesting that the adducted base was in the *syn* conformation about the glycosyl bond, thus allowing the mispaired dA to hydrogen bond with the Hoogsteen face of the modified dG in a G(*syn*):A^+(*anti*) pair. Opposite dT, partial ring-opening was observed, which could facilitate the formation of a dG:dT wobble pair. The ring-closed form of the adduct opposite dT was likely to be *syn*-oriented, placing the exocyclic ring into the major groove to avoid unfavorable steric interactions with the mispaired dT. Further studies are needed to determine whether similar structures could be formed in the active site of the Dpo4 polymerase and why the local sequence context has an unpredictable effect on the mutagenic outcome of the bypass reaction.

Additional types of misinsertions included dGTP with the 5′-CXG-3′ templates and dATP with the 5′-TXG-3′ templates, but these products were observed at low levels relative to the error-free products. The products containing a deletion opposite the adduct sites were also present at very low levels. They could be generated as a result of the formation of type II ternary complexes. Ternary complexes **3** and **4** (Figure 6 and 7) are similar to the "type II" complexes; the incoming nucleotides (dGTP in complex **3** and dATP in complex **4**) skipped the γ-OH-PdG adduct and paired with the 5′-neighboring template nucleotide (dC in complex **3** and dT in complex **4**) utilizing the Watson−Crick geometry. However, these structures are unlikely to represent catalytically active conformations since the 3′-hydroxyl of the primer and the α-phosphate of the incoming nucleotide remained >5.6 Å apart. Thus, consistent with the data of the LC-ESI-MS-MS-based sequencing, the cocrystallization analyses suggested a low probability of replication errors that could be generated via the formation of the type II structures.

■ ASSOCIATED CONTENT

Supporting Information

Mass spectrometric data used for the evaluation of the fidelity of Dpo4-catalyzed replication past the γ-OH-PdG and γ-OH-PdG_{red} lesions. This material is available free of charge via the Internet at http://pubs.acs.org.

■ AUTHOR INFORMATION

Corresponding Author

*Tel: 615-322-2589. Fax: 615-322-7591. E-mail: michael.p.stone@vanderbilt.edu.

Present Addresses

[#]G.S.: Bio-Organic Laboratory, CSIR-Central Leather Research Institute, Adyar, Chennai-600020, India.

[▽]S.B.: Northeastern Collaborative Access Team and Department of Chemistry and Chemical Biology, Cornell University, Building 436E, Argonne National Laboratory, Argonne, IL 60439.

Author Contributions

[⊥]G.S., I.G.M., and S.B. contributed equally to this work.

Funding

This work was supported by NIH Grants P01 ES05355 (to I.D.K., C.J.R., R.S.L., M.E., and M.P.S), P01 CA160032 (to C.J.R., R.S.L., M.E., and M.P.S.), P30 ES00267, Center in Molecular Toxicology; and P30 CA068485, Vanderbilt-Ingram Cancer Center. Vanderbilt University assisted with the purchase of in-house crystallographic instrumentation. Use of the Advanced Photon Source was supported by the U.S. Department of Energy, Office of Science, Office of Basic Energy Sciences, under Contract No. DE-AC02-06CH11357. The LS-CAT Sector 21 beamline is supported by the Michigan Economic Development Corporation and the Michigan Technology Tri-Corridor (Grant 085P1000817).

Notes

The authors declare no competing financial interest.

■ ABBREVIATIONS

γ-OH-PdG, 3-(2′-deoxy-β-D-*erythro*-pentofuranosyl)-5,6,7,8-tetrahydro-8-hydroxypyrimido[1,2-*a*]purin-10(3*H*)-one; PdG, 3-(2′-deoxy-β-D-*erythro*-pentofuranosyl)-5,6,7,8-tetrahydropyrimido[1,2-*a*]purin-10(3*H*)-one; γ-OH-PdG_{red}, reduced γ-OH-PdG (N^2-(3-hydroxypropyl)-dG; Dpo4, DNA polymerase IV from *Sulfolobus solfataricus* P2; LC, liquid chromatography; ESI, electo-spray ionization; MS, mass spectormetry; MALDI-TOF, matrix-assisted laser desorbtion ionization time-of-flight; CID, collision-induced dissociation; M_1dG, 3-(2′-deoxy-β-D-*erythro*-pentofuranosyl)pyrimido[1,2-*a*]purin-10(3*H*)-one.

■ REFERENCES

(1) Burcham, P. C. (1998) Genotoxic lipid peroxidation products: Their DNA damaging properties and role in formation of endogenous DNA adducts. *Mutagenesis 13*, 287−305.

(2) Chung, F. L., Nath, R. G., Nagao, M., Nishikawa, A., Zhou, G. D., and Randerath, K. (1999) Endogenous formation and significance of 1,N^2-propanodeoxyguanosine adducts. *Mutat. Res. 424*, 71−81.

(3) Chung, F. L., Zhang, L., Ocando, J. E., and Nath, R. G. (1999) Role of 1,N^2-propanodeoxyguanosine adducts as endogenous DNA lesions in rodents and humans. *IARC Sci. Publ. 150*, 45−54.

(4) Nair, U., Bartsch, H., and Nair, J. (2007) Lipid peroxidation-induced DNA damage in cancer-prone inflammatory diseases: A review of published adduct types and levels in humans. *Free Radical Biol. Med. 43*, 1109−1120.

(5) Stevens, J. F., and Maier, C. S. (2008) Acrolein: Sources, metabolism, and biomolecular interactions relevant to human health and disease. *Mol. Nutr. Food Res. 52*, 7−25.

(6) Marnett, L. J., Hurd, H. K., Hollstein, M. C., Levin, D. E., Esterbauer, H., and Ames, B. N. (1985) Naturally occurring carbonyl compounds are mutagens in *Salmonella* tester strain TA104. *Mutat. Res. 148*, 25−34.

(7) Curren, R. D., Yang, L. L., Conklin, P. M., Grafstrom, R. C., and Harris, C. C. (1988) Mutagenesis of xeroderma pigmentosum fibroblasts by acrolein. *Mutat. Res. 209*, 17−22.
(8) Smith, R. A., Cohen, S. M., and Lawson, T. A. (1990) Acrolein mutagenicity in the V79 assay. *Carcinogenesis 11*, 497−498.
(9) Kawanishi, M., Matsuda, T., Nakayama, A., Takebe, H., Matsui, S., and Yagi, T. (1998) Molecular analysis of mutations induced by acrolein in human fibroblast cells using *supF* shuttle vector plasmids. *Mutat. Res. 417*, 65−73.
(10) Wang, H. T., Zhang, S., Hu, Y., and Tang, M. S. (2009) Mutagenicity and sequence specificity of acrolein-DNA adducts. *Chem. Res. Toxicol. 22*, 511−517.
(11) Cohen, S. M., Garland, E. M., St. John, M., Okamura, T., and Smith, R. A. (1992) Acrolein initiates rat urinary bladder carcinogenesis. *Cancer Res. 52*, 3577−3581.
(12) Galliani, G., and Pantarotto, C. (1983) The reaction of guanosine and 2′-deoxyguanosine with acrolein. *Tetrahedron Lett. 24*, 4491−4492.
(13) Chung, F. L., Young, R., and Hecht, S. S. (1984) Formation of cyclic 1,N^2-propanodeoxyguanosine adducts in DNA upon reaction with acrolein or crotonaldehyde. *Cancer Res. 44*, 990−995.
(14) Zhang, S., Villalta, P. W., Wang, M., and Hecht, S. S. (2007) Detection and quantitation of acrolein-derived 1,N^2-propanodeoxyguanosine adducts in human lung by liquid chromatography-electrospray ionization-tandem mass spectrometry. *Chem. Res. Toxicol. 20*, 565−571.
(15) de los Santos, C., Zaliznyak, T., and Johnson, F. (2001) NMR characterization of a DNA duplex containing the major acrolein-derived deoxyguanosine adduct γ-OH-1,-N^2-propano-2′-deoxyguanosine. *J. Biol. Chem. 276*, 9077−9082.
(16) Kim, H. Y., Voehler, M., Harris, T. M., and Stone, M. P. (2002) Detection of an interchain carbinolamine cross-link formed in a CpG sequence by the acrolein DNA adduct γ-OH-1,N^2-propano-2′-deoxyguanosine. *J. Am. Chem. Soc. 124*, 9324−9325.
(17) Cho, Y. J., Kim, H. Y., Huang, H., Slutsky, A., Minko, I. G., Wang, H., Nechev, L. V., Kozekov, I. D., Kozekova, A., Tamura, P., Jacob, J., Voehler, M., Harris, T. M., Lloyd, R. S., Rizzo, C. J., and Stone, M. P. (2005) Spectroscopic characterization of interstrand carbinolamine cross-links formed in the 5′-CpG-3′ sequence by the acrolein-derived γ-OH-1,N^2-propano-2′-deoxyguanosine DNA adduct. *J. Am. Chem. Soc. 127*, 17686−17696.
(18) Kouchakdjian, M., Marinelli, E., Gao, X., Johnson, F., Grollman, A., and Patel, D. (1989) NMR studies of exocyclic 1,N^2-propanodeoxyguanosine adducts (X) opposite purines in DNA duplexes: Protonated X(*syn*):A(*anti*) pairing (acidic pH) and X(*syn*):G(*anti*) pairing (neutral pH) at the lesion site. *Biochemistry 28*, 5647−5657.
(19) Singh, U. S., Moe, J. G., Reddy, G. R., Weisenseel, J. P., Marnett, L. J., and Stone, M. P. (1993) ^{1}H NMR of an oligodeoxynucleotide containing a propanodeoxyguanosine adduct positioned in a $(CG)_3$ frameshift hotspot of *Salmonella typhimurium hisD3052*: Hoogsteen base-pairing at pH 5.8. *Chem. Res. Toxicol. 6*, 825−836.
(20) Weisenseel, J. P., Reddy, G. R., Marnett, L. J., and Stone, M. P. (2002) Structure of an oligodeoxynucleotide containing a 1,N^2-propanodeoxyguanosine adduct positioned in a palindrome derived from the *Salmonella typhimurium hisD3052* gene: Hoogsteen pairing at pH 5.2. *Chem. Res. Toxicol. 15*, 127−139.
(21) Yang, I. Y., Hossain, M., Miller, H., Khullar, S., Johnson, F., Grollman, A., and Moriya, M. (2001) Responses to the major acrolein-derived deoxyguanosine adduct in *Escherichia coli*. *J. Biol. Chem. 276*, 9071−9076.
(22) VanderVeen, L. A., Hashim, M. F., Nechev, L. V., Harris, T. M., Harris, C. M., and Marnett, L. J. (2001) Evaluation of the mutagenic potential of the principal DNA adduct of acrolein. *J. Biol. Chem. 276*, 9066−9070.
(23) Kanuri, M., Minko, I. G., Nechev, L. V., Harris, T. M., Harris, C. M., and Lloyd, R. S. (2002) Error prone translesion synthesis past γ-hydroxypropano deoxyguanosine, the primary acrolein-derived adduct in mammalian cells. *J. Biol. Chem. 277*, 18257−18265.
(24) Yang, I. Y., Chan, G., Miller, H., Huang, Y., Torres, M. C., Johnson, F., and Moriya, M. (2002) Mutagenesis by acrolein-derived propanodeoxyguanosine adducts in human cells. *Biochemistry 41*, 13826−13832.
(25) Yang, I. Y., Johnson, F., Grollman, A. P., and Moriya, M. (2002) Genotoxic mechanism for the major acrolein-derived deoxyguanosine adduct in human cells. *Chem. Res. Toxicol. 15*, 160−164.
(26) Minko, I. G., Washington, M. T., Kanuri, M., Prakash, L., Prakash, S., and Lloyd, R. S. (2003) Translesion synthesis past acrolein-derived DNA adduct, γ-hydroxypropanodeoxyguanosine, by yeast and human DNA polymerase η. *J. Biol. Chem. 278*, 784−790.
(27) Minko, I. G., Kozekov, I. D., Kozekova, A., Harris, T. M., Rizzo, C. J., and Lloyd, R. S. (2008) Mutagenic potential of DNA-peptide crosslinks mediated by acrolein-derived DNA adducts. *Mutat. Res. 637*, 161−172.
(28) Moriya, M., Zhang, W., Johnson, F., and Grollman, A. P. (1994) Mutagenic potency of exocyclic DNA adducts: Marked differences between *Escherichia coli* and simian kidney cells. *Proc. Natl. Acad. Sci. U.S.A. 91*, 11899−11903.
(29) Minko, I. G., Kozekov, I. D., Harris, T. M., Rizzo, C. J., Lloyd, R. S., and Stone, M. P. (2009) Chemistry and biology of DNA containing 1,N^2-deoxyguanosine adducts of the α,β-unsaturated aldehydes acrolein, crotonaldehyde, and 4-hydroxynonenal. *Chem. Res. Toxicol. 22*, 759−778.
(30) Washington, M. T., Minko, I. G., Johnson, R. E., Wolfle, W. T., Harris, T. M., Lloyd, R. S., Prakash, S., and Prakash, L. (2004) Efficient and error-free replication past a minor-groove DNA adduct by the sequential action of human DNA polymerases ι and κ. *Mol. Cell. Biol. 24*, 5687−5693.
(31) Minko, I. G., Yamanaka, K., Kozekov, I. D., Kozekova, A., Indiani, C., O'Donnell, M. E., Jiang, Q., Goodman, M. F., Rizzo, C. J., and Lloyd, R. S. (2008) Replication bypass of the acrolein-mediated deoxyguanine DNA-peptide cross-links by DNA polymerases of the DinB family. *Chem. Res. Toxicol. 21*, 1983−1990.
(32) Wolfle, W. T., Johnson, R. E., Minko, I. G., Lloyd, R. S., Prakash, S., and Prakash, L. (2005) Human DNA polymerase ι promotes replication through a ring-closed minor-groove adduct that adopts a *syn* conformation in DNA. *Mol. Cell. Biol. 25*, 8748−8754.
(33) Boudsocq, F., Iwai, S., Hanaoka, F., and Woodgate, R. (2001) *Sulfolobus solfataricus* P2 DNA polymerase IV (Dpo4): An archaeal DinB-like DNA polymerase with lesion-bypass properties akin to eukaryotic pol η. *Nucleic Acids Res. 29*, 4607−4616.
(34) Ling, H., Boudsocq, F., Woodgate, R., and Yang, W. (2001) Crystal structure of a Y-family DNA polymerase in action: A mechanism for error-prone and lesion-bypass replication. *Cell 107*, 91−102.
(35) Zang, H., Goodenough, A. K., Choi, J. Y., Irimia, A., Loukachevitch, L. V., Kozekov, I. D., Angel, K. C., Rizzo, C. J., Egli, M., and Guengerich, F. P. (2005) DNA adduct bypass polymerization by *Sulfolobus solfataricus* DNA polymerase Dpo4. Analysis and crystal structures of multiple base-pair substitution and frameshift products with the adduct 1,N^2-ethenoguanine. *J. Biol. Chem. 289*, 29750−29764.
(36) Wang, Y., Musser, S. K., Saleh, S., Marnett, L. J., Egli, M., and Stone, M. P. (2008) Insertion of dNTPs opposite the 1,N^2-propanodeoxyguanosine adduct by *Sulfolobus solfataricus* P2 DNA polymerase IV. *Biochemistry 47*, 7322−7334.
(37) Eoff, R. L., Stafford, J. B., Szekely, J., Rizzo, C. J., Egli, M., Guengerich, F. P., and Marnett, L. J. (2009) Structural and functional analysis of *Sulfolobus solfataricus* Y-family DNA polymerase Dpo4-catalyzed bypass of the malondialdehyde-deoxyguanosine adduct. *Biochemistry 48*, 7079−7088.
(38) Christov, P. P., Angel, K. C., Guengerich, F. P., and Rizzo, C. J. (2009) Replication past the N^5-methyl-formamidopyrimidine lesion of deoxyguanosine by DNA polymerases and an improved procedure for sequence analysis of in vitro bypass products by mass spectrometry. *Chem. Res. Toxicol. 22*, 1086−1095.
(39) Eoff, R. L., Egli, M., and Guengerich, F. P. (2010) Impact of DNA lesions on translesion synthesis in replicative and bypass polymerases: from structure to kinetics. In *The Chemical Biology of*

DNA Damage (Geacintov, N. E., and Broyde, S., Eds.) pp 299−330, Wiley-VCH, Weinheim, Germany.
(40) Banerjee, S., Brown, K. L., Egli, M., and Stone, M. P. (2011) Bypass of aflatoxin B_1 adducts by the *Sulfolobus solfataricus* DNA polymerase IV. *J. Am. Chem. Soc. 133*, 12556−12568.
(41) Banerjee, S., Christov, P. P., Kozekova, A., Rizzo, C. J., Egli, M., and Stone, M. P. (2012) Replication bypass of the *trans*-4-hydroxynonenal-derived (6*S*,8*R*,11*S*)-1,N^2-deoxyguanosine DNA adduct by the *Sulfolobus solfataricus* DNA polymerase IV. *Chem. Res. Toxicol. 25*, 422−435.
(42) Nechev, L. V., Harris, C. M., and Harris, T. M. (2000) Synthesis of nucleosides and oligonucleotides containing adducts of acrolein and vinyl chloride. *Chem. Res. Toxicol. 13*, 421−429.
(43) Cavaluzzi, M. J., and Borer, P. N. (2004) Revised UV extinction coefficients for nucleoside-5′-monophosphates and unpaired DNA and RNA. *Nucleic Acids Res. 32*, e13.
(44) Otwinowski, Z., and Minor, W. (1997) Processing of X-ray diffraction data collected in oscillation mode. *Acta Crystallogr., Sect. A 276*, 307−326.
(45) Collaborative Computational Project Number 4. The CCP4 suite: Programs for protein crystallography. *Acta Crystallogr., Sect. D* 1994, *50*, 760−763.
(46) French, S., and Wilson, K. (1978) Treatment of negative intensity observations. *Acta Crystallogr., Sect. A 34*, 517−525.
(47) Brunger, A. T., Adams, P. D., Clore, G. M., DeLano, W. L., Gros, P., Grosse-Kunstleve, R. W., Jiang, J. S., Kuszewski, J., Nilges, M., Pannu, N. S., Read, R. J., Rice, L. M., Simonson, T., and Warren, G. L. (1998) Crystallography & NMR system: A new software suite for macromolecular structure determination. *Acta Crystallogr., Sect. D 54*, 905−921.
(48) Cambillau, C., and Roussel, A. (1997) *TURBO FRODO*, version OpenGL.1., Université Aix-Marseille II, Marseille, France.
(49) Vellieux, F. M. D., and Dijkstra, B. W. (1997) Computation of Bhat's OMIT maps with different coefficients. *J. Appl. Crystallogr. 30*, 396−399.
(50) DeLano, W. L. (2008) *The PyMOL Molecular Graphics System*, DeLano Scientific LLC, Palo Alto, CA.
(51) Chowdhury, G., and Guengerich, F. P. (2011) Liquid chromatography-mass spectrometry analysis of DNA polymerase reaction products. *Curr. Protocols Nucleic Acid Chem. 47*, 7.16.1−7.16.11.
(52) Mao, H., Schnetz-Boutaud, N. C., Weisenseel, J. P., Marnett, L. J., and Stone, M. P. (1999) Duplex DNA catalyzes the chemical rearrangement of a malondialdehyde deoxyguanosine adduct. *Proc. Natl. Acad. Sci. U.S.A. 96*, 6615−6620.
(53) Cho, Y. J., Wang, H., Kozekov, I. D., Kurtz, A. J., Jacob, J., Voehler, M., Smith, J., Harris, T. M., Lloyd, R. S., Rizzo, C. J., and Stone, M. P. (2006) Stereospecific formation of interstrand carbinolamine DNA cross-links by crotonaldehyde- and acetaldehyde-derived α-CH_3-γ-OH-1,N^2-propano-2′-deoxyguanosine adducts in the 5′-CpG-3′ sequence. *Chem. Res. Toxicol. 19*, 195−208.
(54) Huang, H., Wang, H., Qi, N., Kozekova, A., Rizzo, C. J., and Stone, M. P. (2008) Rearrangement of the (6*S*,8*R*,11*S*) and (6*R*,8*S*,11*R*) exocyclic 1,N^2-deoxyguanosine adducts of *trans*-4-hydroxynonenal to N^2-deoxyguanosine cyclic hemiacetal adducts when placed complementary to cytosine in duplex DNA. *J. Am. Chem. Soc. 130*, 10898−10906.
(55) Huang, H., Wang, H., Lloyd, R. S., Rizzo, C. J., and Stone, M. P. (2009) Conformational interconversion of the *trans*-4-hydroxynonenal-derived (6*S*,8*R*,11*S*) 1,N^2-deoxyguanosine adduct when mismatched with deoxyadenosine in DNA. *Chem. Res. Toxicol. 22*, 187−200.